



# Technical Note

## Conjugate heat and mass transfer in metal hydride beds in the hydriding process

Zhixiong Guo<sup>1</sup>, Hyung Jin Sung\*

*Department of Mechanical Engineering, Korea Advanced Institute of Science and Technology, Yusong, Taejon, 305-701, Korea*

Received 2 August 1996; in final form 9 January 1998

### 1. Introduction

Metal hydride applications span a wide variety of technologies, e.g., energy conversion, chemical compressors and hydrogen storage. A knowledge of heat and mass transfer in a metal hydride reactor during the absorption and desorption of hydrogen is important for performance optimization of the reactor. One of the key requirements in the design of metal hydride bed is the enhancement of the effective thermal conductivity of metal hydride powders [1–3]. A literature survey reveals that many attempts have been made to analyze the hydride dynamic character during the absorption/desorption process [1–6]. The main factors governing the dynamics of the metal hydride bed are [4]: heat transfer from/to hydration zone, hydrogen filtration through the metal hydride matrix and kinetics of the hydrogen sorption processes, etc.

As to the heat transfer from/to the metal hydride bed, a major concern is the limited reacting rate process, because of its fast kinetics and low hydride thermal conductivity [1, 2]. To increase the lower thermal conductivity of the bed, several methods have been proposed, e.g., addition of a wire, employment of metal powder of high thermal diffusivity, and use of an aluminum foam matrix to contain the hydride particles. The installation of internal plates, among others, is considered in the present study to enhance the lower thermal conductivity and to improve the reaction dynamics. One of the central ingredients in the present modeling is the treatment of the conjugate nature of heat and mass transfer, which is

applicable to the metal hydride bed. This accounts for the hydration kinetics, hydrogen flow and heat transfer in the hydride powder as well as in the sheets. Another consideration of the reaction process limitation should be given to the hydrogen flow, which depends on the thickness of the bed [2]. The majority of past endeavors has considered a unique thickness of the bed.

In the present treatise, an unsteady two-dimensional model is developed, which takes into account the hydrogen flow, reaction kinetics, and conjugate heat transfer in the metal hydride and aluminum sheet regions. The nonlinear coupled differential equations are solved numerically by an iterative method based on the control-volume technique. The heat transfer enhancement by the aluminum sheets and the optimization of the operation of hydride bed are examined. The present numerical simulation can predict the time-space evolution of concentration, pressure and temperature in the bed. The influences of the thickness of the bed and the interval gap distance between sheets are evaluated. The main efforts are focused on the improvement of the reaction rate.

### 2. Mathematical model

A physical model of the flow and heat and mass transfer in a metal hydride bed is sketched in Fig. 1. It consists of a quantity of hydride particles, a screen, a wall, and aluminum (Al) sheets of thickness  $\delta$  connecting the screen and the wall. A solid phase metal hydride is packed in the enclosed region with the gaseous phase hydrogen. The temperature of the wall is maintained at a prescribed value  $T_0$ . The inlet pressure is  $P_i$ . The gap distance between Al sheets is  $H$  and the thickness of the bed is  $L$ . Although a large number of sheets are inserted into the

---

\* Corresponding author. Tel.: 00 82 42 869 3027; Fax: 00 82 42 869 5027; E-mail: hjsung@cais.kaist.ac.kr

<sup>1</sup> Present address: Institute of Fluid Science, Tohoku University, Sendai 980, Japan.

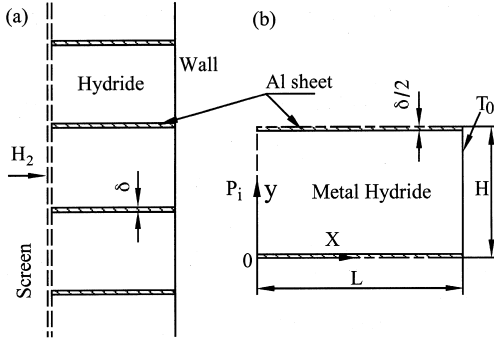


Fig. 1. (a) Physical model of hydride bed; (b) calculation domain.

bed, only one element shown in Fig. 1(b) is considered in the present analysis.

Before the formulation of the governing equations, the following assumptions are adopted for simplicity [2, 5]: (1) the hydrogen behaves as an ideal gas; (2) the metal hydride is homogeneous, isotropic and in local thermal equilibrium; (3) the hydride density is constant. The governing equations based on the 'local volume averaging' technique [4] are established. The gas phase conservation equation is

$$\frac{\partial}{\partial t}(\varepsilon \langle \rho_\gamma \rangle) + \nabla \cdot (\langle \rho_\gamma \rangle \langle \mathbf{v} \rangle) = -\langle \dot{m} \rangle, \quad (1)$$

where  $\langle \dot{m} \rangle$  denotes the volumetric mass rate of hydrogen absorption and  $\varepsilon$  is the porosity of the powder.  $\mathbf{v}$  is the velocity vector and  $\langle \rho_\gamma \rangle$  represents the density of gas phase. The notation  $\langle \rangle$  represents the local volume averaging and the subscript  $\gamma$  represents gas phase. Darcy's law is employed in the equation of motion in the gas phase [1, 3, 4]

$$\nabla \langle P_\gamma \rangle = -\frac{\mu}{K_{\text{eff}}} \langle \mathbf{v} \rangle \quad (2)$$

where

$$K_{\text{eff}} = K_D(1 + 1.15Kn) \quad (3)$$

$$K_D = \frac{d_p^2 \varepsilon^3}{180(1-\varepsilon)^2}, \quad Kn = \frac{\lambda}{L_c} \quad (4)$$

$$L_c = \sqrt{K_D}, \quad \lambda = \frac{\mu}{\langle P_\gamma \rangle} \sqrt{\frac{\pi \Re \langle T_\gamma \rangle}{2M_\gamma}}. \quad (5)$$

Here,  $K_{\text{eff}}$  is the effective permeability [2],  $d_p$  the averaged diameter of particles,  $M$  the molecular weight,  $P$  the pressure,  $\Re$  the universal gas constant,  $T$  the temperature and  $\mu$  the dynamic viscosity, respectively. As the particle size is distributed from 1–100  $\mu\text{m}$  [5], the Knudsen number is usually in the range  $Kn < 1$  for metal hydride powders. Thus, the hydrogen flow is mainly in the tran-

sitional or continuum regime. Substitution of equation (2) into equation (1), using the ideal gas state equation, leads to

$$\frac{\partial}{\partial t} \left( \frac{\varepsilon M_\gamma}{\Re T} \langle P_\gamma \rangle \right) = \nabla \cdot \left( \frac{K_{\text{eff}} M_\gamma}{\mu \Re T} \langle P_\gamma \rangle \nabla \langle P_\gamma \rangle \right) - \langle \dot{m} \rangle. \quad (6)$$

The energy conservation equation in metal hydride is

$$\rho_b (C_p)_\sigma \frac{\partial T}{\partial t} + \langle \rho_\gamma \rangle (C_p)_\gamma \langle \mathbf{v}_\gamma \rangle \cdot \nabla T = \nabla \cdot (k_{\text{eff}} \nabla T) + \langle \dot{Q} \rangle \quad (7)$$

in which local thermal equilibrium is assumed [2, 5]. The density of the bed is expressed by  $\rho_b = (1-\varepsilon)\rho_\sigma$  and  $k_{\text{eff}}$  is the effective thermal conductivity of the bed. The chemical reaction heat rate is  $\langle \dot{Q} \rangle = -\langle \dot{m} \rangle \Delta H / M_\gamma$ . The subscript  $\sigma$  represents the solid phase and  $C_p$  is the specific heat capacity. The heat conduction equation in the sheets is written as

$$\rho_a (C_p)_a \frac{\partial T}{\partial t} = \nabla \cdot (k_a \nabla T). \quad (8)$$

The kinetics of the hydrogen absorption and desorption is described in terms of a shrinking core model [6]. The core is taken to be a saturated  $\alpha$ -phase metal, while hydride is the  $\beta$ -phase. Hence, the effective heat capacity is  $(C_p)_\sigma = (1-C) \cdot C_a + C \cdot C_\beta$ , in which  $C$  represents the atomic ratio of the bounded hydrogen to the metal hydride. The concentration reaction rate is obtained from the following expression [2, 4]

$$\langle \dot{C} \rangle = D \cdot \exp \left( -\frac{E_a}{\Re T} \right) \frac{\langle P_\gamma \rangle^{1/2} - P_{\text{eq}}^{1/2}}{(1-\omega)^{-1/3} - 1} \quad (9)$$

where  $\omega = C/C_{\text{max}}$ , and  $D$  is the diffusion parameter determined by a best fit to the experimental data.  $E_a$  represents the activation energy. The equilibrium pressure  $P_{\text{eq}}$  is related to the van't Hoff equation. The modified equation of Nishizaki et al. [7] is employed for  $P_{\text{eq}}$ :

$$\ln \left( \frac{P_{\text{eq}}}{1.0133 \times 10^5} \right) = \frac{\Delta H}{\Re T} - \frac{\Delta S}{\Re} + (\phi \pm \phi_0) \tan \left[ \pi \left( \omega - \frac{1}{2} \right) \right] \pm \frac{\beta}{2} \quad (10)$$

where  $\Delta H$  is the heat of formation and  $\Delta S$  is the entropy change.  $\beta$  and  $\phi$  are the plateau hysteresis factor and the plateau flatness factor, respectively. The volumetric mass reaction rate  $\langle \dot{m} \rangle$  is then calculated by

$$\langle \dot{m} \rangle = \langle \dot{C} \rangle \frac{M_H (1-\varepsilon) \rho_\sigma}{M_\sigma}. \quad (11)$$

The initial condition is set as

$$t = 0: \quad T = T_0, \quad C = C_0, \quad \langle P_\gamma \rangle = P_{\text{eq}}(\omega_0, T_0) \quad (12)$$

and the boundary conditions are

$$x = 0: \quad \langle P_\gamma \rangle = P_i, \quad -k_{\text{eff}} \frac{\partial T}{\partial x} = \langle \rho_\gamma \rangle \langle u \rangle (C_p)_\gamma (T - T_0) \quad (13)$$

$$x = L: \quad \frac{\partial \langle P_\gamma \rangle}{\partial x} = 0, \quad T = T_0 \quad (14)$$

$$y = 0 \quad \text{or} \quad y = H: \quad \frac{\partial \langle P_\gamma \rangle}{\partial y} = 0, \quad \frac{\partial T}{\partial y} = 0. \quad (15)$$

In the above,  $\langle u \rangle$  represents the velocity component in the  $x$ -direction. The second boundary condition in equation (13) satisfies the requirement of continuity of the energy flux at  $x = 0$ , while the second boundary condition in equation (14) ignores the possibility of a contact resistance between the wall and the powder bed.

A fully implicit scheme based on the control-volume formulation [8] was introduced to discretize the governing equations. A harmonic-mean formulation was adopted for the interface diffusion coefficients between two control volumes. This approach is capable of handling the abrupt changes in these coefficients at the hydride/sheet interface [9]. The resulting algebraic equations were solved by the tridiagonal matrix algorithm [8]. The spatial grid was varied from  $100 \times 40$  to  $200 \times 160$  in the  $x$ - $y$  computational domain shown in Fig. 1(b). The time step was set to be 0.1 s, while during the first 5 s of the reaction, the time increment was changed from 0.001–0.1 s in order to capture the sudden change of chemical reaction. The calculation was iterated at the same time-step until the relative variations of pressure and of temperature between two successive iterations were smaller than the prearranged accuracy levels of  $10^{-4}$ . The numerical results were validated by checking them against the experiment [1] with good agreement.

### 3. Results

The calculated metal hydride reaction bed is filled inside a glove-box with fully activated  $\text{LaNi}_{4.7}\text{Al}_{0.3}$  powder to the appropriate bed thickness. The hydride properties of the present calculations are set forth [7]:  $\Delta H = -33,819.7 \text{ J mol}_{\text{H}_2}^{-1}$ ,  $\Delta S = -107.41 \text{ J mol}_{\text{H}_2}^{-1} \text{ K}^{-1}$ ,  $\phi = 0.30$ ,  $\phi_0 = 0.005$ ,  $\beta = 0.098$ ,  $\varepsilon = 0.5$ ,  $\rho_b = 2500 \text{ kg m}^{-3}$ ,  $C_\alpha = 339.67 \text{ J kg}^{-1} \text{ K}^{-1}$ ,  $C_\beta = 492.1 \text{ J kg}^{-1} \text{ K}^{-1}$ ,  $d_p = 0.03 \text{ mm}$ ,  $E_a = 33.9 \text{ kJ mol}_{\text{H}_2}^{-1}$ ,  $k_{\text{eff}} = 1.3 \text{ W m}^{-1} \text{ K}^{-1}$  and  $C_{\text{max}} = 1.0$ . A value of  $D = 14.89 \times 10^{-6}$  in equation (9) is deemed to give a suitable match with the experiment of Supper et al. [1]. The properties of the aluminum sheet are  $(C_p)_a = 903 \text{ J kg}^{-1} \text{ K}^{-1}$ ,  $k_a = 220 \text{ W m}^{-1} \text{ K}^{-1}$  and  $\rho_a = 2699 \text{ kg m}^{-3}$ . The hydride has an initial hydrogen concentration  $C_0 = 0.1$  for hydriding processes. The thickness of the aluminum sheet is  $\delta = 0.1 \text{ mm}$ . The inlet pressure and initial temperature are set as  $P_i = 3 \text{ atm}$  and  $T_0 = 293 \text{ K}$  in the present simulation, respectively.

The influence of the installation of aluminum sheets

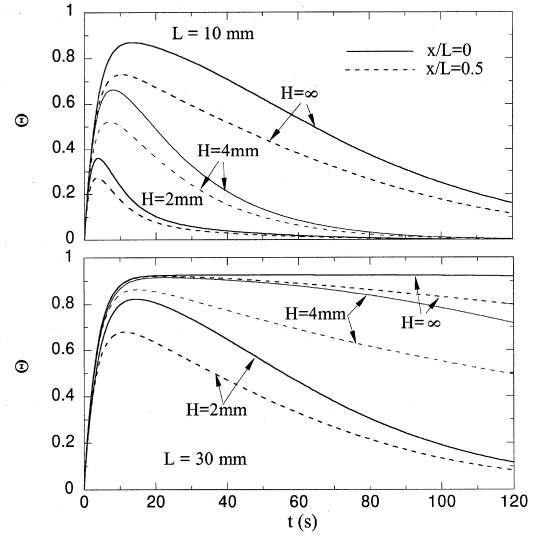


Fig. 2. Temperature distributions as a function of charging time for different  $H$ .  $L = 10 \text{ mm}$ ,  $30 \text{ mm}$ .  $P_i = 3 \text{ atm}$  and  $T_0 = 293 \text{ K}$ .

on heat transfer of the reactor is demonstrated in Fig. 2. Two cases of the thickness of the bed are selected, i.e.,  $L = 10 \text{ mm}$  and  $L = 30 \text{ mm}$ . The dimensionless temperature is defined as  $\theta = (T - T_0)/(T_{\text{eq}0} - T_0)$ , where  $T_{\text{eq}0}$  is the van't Hoff's equilibrium temperature at  $P_i$  and  $\omega = 0.5$ . When no aluminum sheet is installed,  $H = \infty$ . The solid line represents the temperature at the screen ( $x/L = 0$ ), while the dashed line is the temperature at the center location of the bed ( $x/L = 0.5$ ). The value at each position is an averaged one along the  $y$ -direction in the initial stage due to the reaction caused by the inlet high pressure, and it then decreases slowly. Obviously, the temperature with aluminum sheets is lower than that without aluminum sheets ( $H = \infty$ ). As the gap distance becomes smaller, i.e.,  $H$  decreases, the temperature decreases. This means that the heat transfer in the metal hydride bed can be significantly enhanced by the insertion of Al sheets.

To look into the influence of the sheet insertion on the reaction rate, the profiles of hydrogen mass absorbed as a function of time are exhibited in Fig. 3. The reaction time is usually considered as that of hydrogen absorbed reaches 80% of the maximum hydrogen absorbed without Al sheet [2]. It is noticed that the reaction time is decreased when the number of sheets increases (small  $H$ ), i.e., the reaction rate is augmented as the heat transfer is enhanced. However, an optimal value of  $H$  exists. When  $H$  is smaller than the optimal value, a reverse effect occurs. This can be explained from equation (9) that the reaction rate  $\langle \dot{C} \rangle$  is proportional to  $\exp(-E_a/\mathcal{R}T) \cdot (\langle P_\gamma \rangle^{1/2} - P_{\text{eq}}^{1/2})$ . As  $T$  decreases due to the insertion of Al sheets, the first term  $\exp(-E_a/\mathcal{R}T)$  decreases, while the

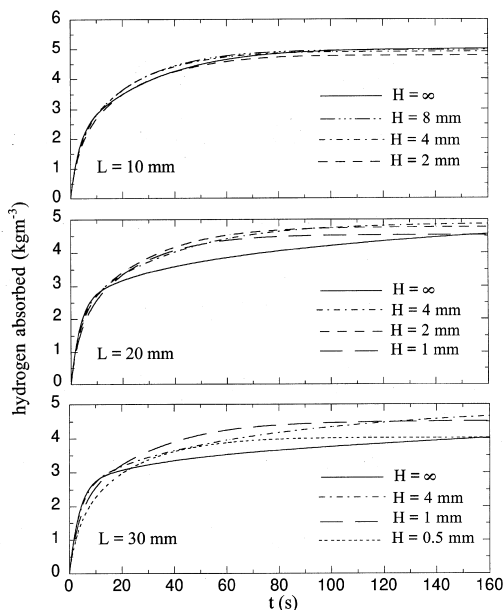


Fig. 3. Influences of  $H$  and  $L$  on the total mass absorbed.  $P_i = 3$  atm and  $T_0 = 293$  K.

second term ( $\langle P_\gamma \rangle^{1/2} - P_{eq}^{1/2}$ ) increases according to equation (10). However, after an optimal point is achieved, as the number of sheets increases further, the decrease of the first term  $\exp(-E_a/RT)$  becomes larger than the increase of the second term. Accordingly, the reaction rate is decreased. The thickness of the reactor also plays an important role in the heat transfer of metal hydride bed, which in turn affects the reaction. Inspection of Fig. 3 for three beds ( $L = 10, 20$  and  $30$  mm) reveals that the optimal value of  $H$  decreases as the thickness of the beds increases. This means the influence of aluminum sheet on the reaction rate becomes more noticeable in thicker hydride beds. In other words, as the bed thickness increases, the limitation of heat transfer is more important. This phenomenon can be explained by Fig. 2, in which the denser packed Al sheets are required in order to remove the reaction generated heat inside the thicker beds.

#### 4. Conclusions

Detailed numerical analyses were performed to delineate the unsteady two-dimensional conjugate heat and mass transfer characteristics in a metal hydride bed. The main emphasis was placed on the heat transfer enhancement as well as the improvement of the reaction rate by the addition of aluminum sheets. The results indicated that the heat transfer and the reaction rate can be significantly augmented by the insertion of aluminum sheets. As the aluminum sheets are densely packed, i.e.,  $H$  decreases, the heat transfer is augmented and the reaction rate increases. However, an optimal  $H$  exists for achieving the fastest reaction rate. The thickness of the reactors also plays an important role in the heat transfer of metal hydride bed. The optimal value of  $H$  decreases as the thickness of the beds increases.

#### References

- [1] W. Supper, M. Groll, U. Mayer, Reaction kinetics in metal hydride reaction beds with improved heat and mass transfer, *J. Less-Common Metals* 104 (1984) 279–286.
- [2] H. Choi, A.F. Mills, Heat and mass transfer in metal hydride beds for heat pump applications, *Int. J. Heat Mass Transfer* 33 (1990) 1281–1288.
- [3] S.G. Lee, H.H. Lee, K.Y. Lee, J.Y. Lee, Dynamic reaction characteristics of the tubular hydride bed with large mass, *J. Alloys and Compounds* 235 (1996) 84–92.
- [4] A.V. Kuznetsov, K. Vafai, Analytical comparison and criteria for heat and mass transfer models in metal hydride packed beds, *Int. J. Heat Mass Transfer* 38 (1995) 2873–2884.
- [5] A. Isselhorst, Heat and mass transfer in coupled hydride reaction beds, *J. Alloys and Compounds* 231 (1995) 871–879.
- [6] M.Y. Song, J.Y. Lee, A study of the hydriding kinetics of Mg-(10–20w/o)LaNi<sub>5</sub>, *Int. J. Hydrogen Energy* 8 (1983) 363–367. *J. Alloys and Compounds* 231 (1995) 670–674.
- [7] T. Nishizaki, K. Miyamoto, K. Yoshida, Coefficients of performance of hydride heat pumps, *J. Less-Common Metals* 89 (1983) 559–566.
- [8] S.V. Patankar, *Numerical Heat Transfer and Fluid Flow*, Hemisphere, New York, 1980, p. 149.
- [9] Z. Guo, H.J. Sung, J.M. Hyun, Pulsating flow and heat transfer in an annulus partially filled with porous media, *Numer. Heat Transfer, Part A* 31 (1997) 517–527.